ARCHIVES OF BIOCHEMISTRY AND BIOPHYSICS
Vol. 301, No. 1, February 15, pp. 184–189, 1993

Hydrogen Peroxide-Dependent Formation and Bleaching of the Higher Oxidation States of Bovine Erythrocyte Green Hemeprotein[1]

Feng Xu, Louis J. DeFilippi,[2] David P. Ballou, and Donald E. Hultquist[3]
Department of Biological Chemistry, The University of Michigan, Ann Arbor, Michigan 48109-0606

Received August 31, 1992, and in revised form November 2, 1992

The ferric and ferrous forms of bovine erythrocyte green hemeprotein react with hydroperoxides to form higher oxidation state intermediates with absorbance maxima in the Soret region at 426 and 422 nm, respectively. In the absence of an appropriate reductant, these intermediates undergo rapid bleaching reactions. 2,2'-Azinobis(3-ethylbenzthiazoline-6-sulfonic acid) rapidly reduces the intermediate formed by reaction of ferric green hemeprotein with hydrogen peroxide, thereby preventing bleaching and allowing the rate of the intermediate formation to be calculated from the coupled dye oxidation. This rate constant of 70 M^{-1} s^{-1} at 23°C is similar to those determined by bleaching and by direct photometric detection of the intermediate. Dihydroriboflavin rapidly reduces the intermediate formed by reaction of ferrous green hemeprotein with hydrogen peroxide, thereby preventing bleaching and allowing the rate of the intermediate formation to be calculated from the coupled dihydroriboflavin oxidation; the rate constant of 2×10^4 M^{-1} s^{-1} at 23°C is similar to the value calculated by direct detection of the intermediate. The results demonstrate that, in contrast to the reductase activity of its heme-free form, the green heme form of the protein reacts with hydroperoxides to generate highly unstable peroxide complexes.

A green hemeprotein (GHP)[4] with a unique prosthetic group has been isolated from human erythrocytes and two spectrally distinct forms of the hemeprotein have been isolated from bovine erythrocytes (1–5). Immunological methods have detected the protein in rat and rabbit erythrocytes and in bovine and rat liver (6). In bovine erythrocytes, the concentration of this protein has been estimated to be 10 μM; of the hemeproteins isolated from bovine erythrocytes, only hemoglobin has been isolated in larger amounts. When protein purification is carried out in the presence of dithiothreitol, an apoprotein form of the protein is isolated from human, bovine, and bullfrog erythrocytes, and this form of the protein has been characterized in terms of its reductase activity (6–9). The protein moieties of the bovine and bullfrog erythrocyte proteins have been subjected to partial amino acid sequencing (8, 9). The heme-free form of the bovine protein has recently been shown to be a binding protein with affinity toward hemes, porphyrins, and fatty acids (6).

Among hemeproteins, GHP exhibits an especially striking reactivity toward oxidizing agents. In its ferrous state, the hemeprotein very rapidly reduces dioxygen to superoxide anion; both the ferric and the ferrous forms of the hemeprotein undergo bleaching in the presence of hydroperoxides (10). The role of hemeproteins in stimulating cellular oxidative damage is under intensive investigation (11–16). The reactions of hemeproteins with peroxide to generate highly reactive oxy radicals and hemeprotein higher oxidation states have been postulated to be responsible for both the inactivation of enzymes and the disruption of cellular organization. The present work was undertaken to gain a quantitative and mechanistic understanding of the reactions of GHP with hydrogen peroxide with the hope of obtaining insight into the biological function of this protein.

EXPERIMENTAL PROCEDURES

Materials. Metmyoglobin (horse heart, IGM) was obtained from ICN, riboflavin from Eastman, hydrogen peroxide (30%) from EM Science, ethyl hydroperoxide (11%) from Polysciences; 2,2'-azino-bis(3-ethylbenzthiazoline-6-sulfonic acid) diammonium salt (ABTS), horseradish peroxidase (HRP), type XII, and cytochrome *c* (horse heart, type III)

[1] This work was supported in part by NIH Research Grants AG-07046 and GM-02877 and a grant from the Office of the Vice President of Research, The University of Michigan.

[2] Present address: Biotechnology Department, Allied-Signal Research & Technology, Des Plaines, IL 60017-5016.

[3] To whom correspondence should be addressed. Fax: (313) 763-4581.

[4] Abbreviations used: ABTS, 2,2'-azinobis(3-ethylbenzothiazoline-6-sulfonic acid); GHP-I and GHP-II, green hemeprotein forms I and II; HRP, horseradish peroxidase.

0003-9861/93 $5.00

were from Sigma. The two forms of bovine erythrocyte green hemeprotein (GHP-I and GHP-II) were purified as described previously (3).

General methods. Spectral measurements were conducted on either a Kontron Uvikon 810 spectrophotometer, using a quartz cuvette of 1-cm light path, or a stopped-flow instrument (built such that no metal parts are in contact with the solution), using a quartz cuvette of 2-cm light path (17). Photometric titrations were performed by monitoring absorbance at the Soret band maxima, using potassium phosphate buffers for pH 3 and the pH 6–8 range, sodium acetate buffers for the pH 3.5–6 range, Tris chloride buffers for the pH 8–9 range, and sodium carbonate buffers for the pH 9–11 range. Ferrous GHP was prepared from ferric GHP by photochemical reduction using a 1:100 molar ratio of riboflavin to GHP (10, 18).

Peroxidative reactions of ferric green hemeprotein. The reaction of ferric GHP with H_2O_2 or ethyl hydroperoxide, to generate an intermediate, and the subsequent bleaching events were measured at 3°C by spectrophotometry between 390 and 470 nm using 1.7 μM GHP and 2–16 mM peroxides in 50 mM buffer, pH 8.4. At 23°C the bleaching of ferric GHP was carried out with 1–3 μM GHP and 1–20 mM H_2O_2 in 50 mM buffer, pH 7.2, by monitoring the decay of the Soret band.

The formation of the intermediate from ferric GHP and H_2O_2 was also measured by coupling the reaction to the oxidation of ABTS, in what constitutes a peroxidase activity (19). Typical reaction mixtures contained 0.05–0.50 μM GHP, 0.02–0.30 mM H_2O_2, 0.4–4.0 mM ABTS, and 30–100 mM buffer. The reactions were started by adding H_2O_2 and monitored by following the increase in absorbance of the ABTS radical cation at 660 nm (ϵ = 12 mM^{-1} cm^{-1}). In the absence of GHP, the oxidation of ABTS by H_2O_2 was barely detectable in the experimental time frame. The same ABTS coupling system was used to measure the peroxidations of horseradish peroxidase (2.3–23 nM), metmyoglobin (0.6–3.0 μM), and ferricytochrome c (1.6–16 μM).

Peroxidative reactions of ferrous green hemoprotein. The direct measurement of the intermediate formation from ferrous GHP and H_2O_2 and the subsequent bleaching were studied with 3.5 μM ferrous GHP and 0.03–0.24 mM H_2O_2 in 10 mM buffer, pH 8.4, at 17°C by monitoring the spectrum between 390 and 510 nm using the stopped-flow technique.

Formation of intermediate from ferrous GHP and H_2O_2 was measured by coupling the reaction to the oxidation of dihydroriboflavin, according to a recently developed procedure that measures the rate of formation of ferryl derivatives from ferrous hemeprotein and H_2O_2 (20). Typical reaction mixtures contained 0.07–0.8 μM GHP, 10–40 μM riboflavin, 0.98 mM EDTA, 1–10 μM H_2O_2, and 3 mM buffer. After the samples were made anaerobic, they were photochemically reduced (10) and then mixed with an aliquot of anaerobic H_2O_2 solution to give a final H_2O_2 concentration of 0.5–5 μM. The coupled reaction was monitored by following the oxidation of riboflavin at 450 nm ($\Delta\epsilon$ = 11 mM^{-1} cm^{-1}). Rate constants were calculated from the dependence of initial rate and of overall half-life on the concentration of reactants. A correction was made for the direct reaction of dihydroriboflavin with H_2O_2.

RESULTS

Catalysis of peroxidation reactions. Ferric GHP catalyzes the oxidation of ABTS by H_2O_2 to form ABTS radical cation (Fig. 1A). Under the experimental conditions described above, this reaction exhibits an exponential-type time course, with initial rates depending on both GHP and H_2O_2 concentrations and half-life depending only on GHP concentration. An example of the initial linear part of the ABTS cation radical formation profile is shown in Fig. 1B. Second-order rate constants derived from the overall half-life and from the initial rate are in close agreement. This ABTS coupling method at pH 7.2 and 23°C yields second-order rate constants of 69 and 64 M^{-1} s^{-1} for GHP-I and GHP-II, respectively. In comparison, the method yields larger values for the second-order rate constants of HRP and metmyoglobin and a smaller value for ferricytochrome c (Table I). When GHP in assay solutions is sufficiently concentrated to allow spectral detection, the GHP is observed to remain unchanged in its

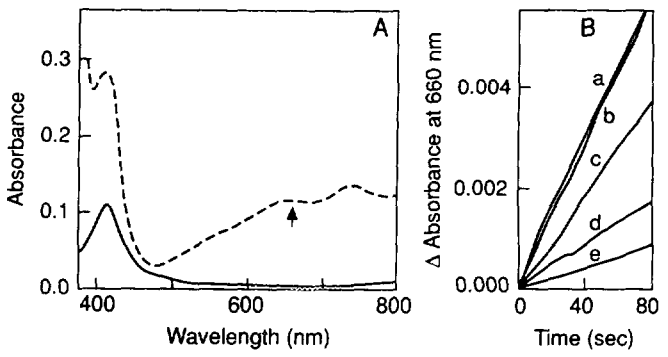

FIG. 1. Spectral changes resulting from the catalysis by ferric GHP-I of the peroxidation of ABTS. (A) Spectra of a solution containing 1.2 μM ferric GHP-I and 0.54 mM ABTS in 83 mM buffer, pH 7.2. (—) Before the addition of H_2O_2; (- - -) 1 h after the solution was made 2.1 μM in H_2O_2. Arrow identifies the wavelength (660 nm) used to follow the reactions shown in (B). (B) Initial time courses of the reaction as measured by change of absorbance at 660 nm in 0.1 M buffer, pH 7.2. a, 0.75 μM ferric GHP-I, 2 mM ABTS, and 51 μM H_2O_2; b, 0.75 μM ferric GHP-I, 1 mM ABTS, and 51 μM H_2O_2; c, 0.75 μM ferric GHP-I, 1 mM ABTS, and 35 μM H_2O_2; d, 0.75 μM ferric GHP-I, 1 mM ABTS, and 18 μM H_2O_2; e, 0.33 μM ferric GHP-I, 0.4 mM ABTS, and 15 μM H_2O_2.

TABLE I

Second-Order Rate Constants for Reactions of GHP with H_2O_2

Form of GHP	k (M^{-1} s^{-1})
Ferric GHP-I	69,[a] 44,[b] 13[c]
Ferric GHP-II	64,[a] 59[b]
Ferric HRP	8×10^6,[a] 10^7,[d] $\sim 2 \times 10^6$ [e]
Ferric myoglobin	580,[a] 130,[f] 140[g]
Ferric cytochrome c	4,[a] ~ 10[a,h]
Ferrous GHP-I	2.3×10^4,[i] 1.2×10^4 [j]
Ferrous GHP-II	1.9×10^4 [i]
Ferrous myoglobin[k]	7.5×10^4 [i]

[a] Determined in a coupled ABTS reaction at 23°C, pH 7.2 (this study).
[b] Determined from the bleaching reaction at 23°C, pH 7.2 (this study).
[c] k_2/K'_m value for the formation of Intermediate I at 3°C, pH 8.4 (this study).
[d] Determined for the formation of Compound I at room temperature, pH 7.0 (23).
[e] Calculated from the initial rate of the coupled ABTS reaction at 20°C, pH 6 .0 (19).
[f] Determined in a coupled ABTS reaction at 23°C, pH 8.5 (this study).
[g] Determined from the direct reaction with H_2O_2 at 23°C, pH 8.5 (24).
[h] Estimated from the V_{max}/K_m at 18°C, pH 7.0 (25).
[i] Determined in a coupled reaction with dihydroriboflavin at 23°C, pH 7.2 (this study).
[j] k_2/K'_m value determined for formation of Intermediate II at 17°C, pH 8.4 (this study).
[k] Determined in a coupled reaction with dihydroriboflavin at 23°C, pH 7.2 (20).

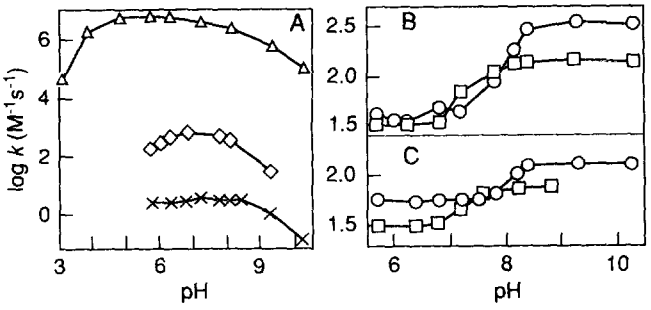

FIG. 2. pH profiles of ABTS peroxidase activity and bleaching reactions of ferric GHP. Log of the second-order rate constant, log k (M^{-1} s^{-1}), is plotted versus pH. For details see Experimental Procedures. (A) Peroxidase activities of: △, HRP; ◇, metmyoglobin; ×, cytochrome c. (B) Peroxidase activities of: □, GHP-I; ○, GHP-II. (C) Bleaching reactions of: □, GHP-I; ○, GHP-II.

TABLE II

pK_a Values from Photometric Titrations and pH Profiles of Rate Constants

Protein	Ferrous	Ferric		
	Photometric titration	Photometric titration	pH profile of ABTS oxidation	pH profile of H_2O_2 bleaching
GHP-I	4.2	4.8, 9.0	6.7, 7.4	6.8, 7.5
GHP-II	4.9	5.2, 8.9	7.4, 8.4	7.7, 8.3
cyt c	[a]	2.5,[b] 9.6[b]	8.9	
Mb	[a]	4.0, 9.0[c]	6.3, 8.0	
HRP		2.6, 11.0[d]	4.0, 8.4	

[a] No acid–base transition seen between pH 3 and 9.
[b] Agrees with the published values of 2.5 and 9.4 (29).
[c] Agrees with the published value of 8.9 (30).
[d] Agrees with the published value of 11.0 (22).

ferric form throughout the course of the reaction, as demonstrated by the absorbance at the Soret peak of GHP in Fig. 1A. For each of the hemeproteins studied, the final concentration of ABTS cation radical is proportional to the initial H_2O_2 concentration; the molar equivalents of ABTS radical cation generated per mole of added H_2O_2 was calculated to be 2.0 ± 0.3, as is the case in Fig. 1A. The spectral change due to the formation of ABTS cation radical stabilizes after H_2O_2 is depleted. The pH profiles of the ABTS peroxidase activity of GHP are shown in Fig. 2B, and the contrasting results obtained with HRP, metmyoglobin, and ferricytochrome c are shown in Fig. 2A. The pK_a values derived from the pH profiles are presented in Table II.

In a parallel fashion and under the same conditions, ferrous GHP catalyzes the oxidation of dihydroriboflavin to riboflavin by H_2O_2 (Fig. 3). From measurements of the concentration dependence of initial absorbance change and half-life of the overall reaction, the reaction was found to be first-order with respect to H_2O_2 and GHP, and zero-order with respect to dihydroriboflavin. The second-order rate constants determined by this coupling method for GHP-I and GHP-II at pH 7.2 are 2.3×10^4 and 1.9×10^4 M^{-1} s^{-1}, respectively (Table I). The rate constants do not change appreciably over the pH range of 3 to 9. Adding an aliquot of H_2O_2 generates 1.0 ± 0.2 molar equivalent oxidized riboflavin, as shown in Fig. 3A. With dihydroriboflavin in excess over H_2O_2, the position of the Soret band of the ferrous GHP remains essentially unchanged throughout the reaction until H_2O_2 is depleted.

Formation and subsequent bleaching of the higher oxidation states of GHP. In contrast to the coupled reactions with ABTS, in the absence of ABTS the ferric forms of GHP-I and GHP-II bleach upon reaction with either H_2O_2 or ethyl hydroperoxide, yielding products with no absorbance in the Soret or visible regions (Ref. 10 and Fig. 4A). GHP bleaching is not prevented by reductants less reactive than ABTS, such as ascorbate (15 μM), 2,3,5,6-tetramethylphenylenediamine (10 mM), *N,N'*-dimethylphenylenediamine (0.3 mM), dichloroindophenol (0.2 mM), biliverdin (12 μM), tryptophan (10 μM), or tyrosine (0.8 mM). Initial rates of bleaching were found to depend only on the concentrations of GHP and H_2O_2. Figures 2B and 2C show the similarity at 23°C between the pH profiles of the bleaching rates for the GHP-H_2O_2 systems and the pH profiles of the coupled peroxidative reactions.

When ferric GHP-I is mixed with H_2O_2 at 3°C and pH 8.4, a biphasic reaction is observed, indicating formation of an intermediate, "Intermediate I," before final bleaching occurs (Fig. 4B). Figure 4A shows a spectrum (dashed line), obtained when the intermediate reaches a maximum

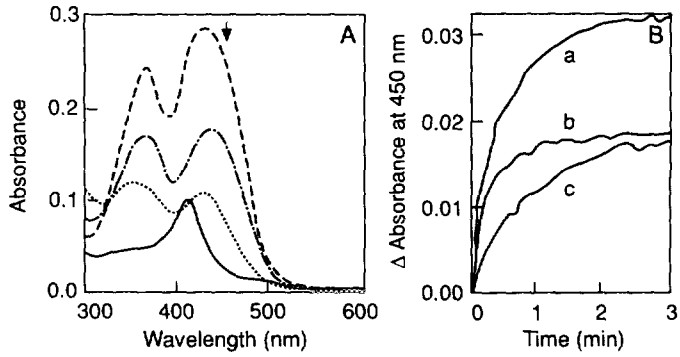

FIG. 3. Spectral changes resulting from the catalysis of dihydroriboflavin peroxidation by ferrous GHP-II. A. Spectra of a solution containing 1.2 μM GHP-II in 34 mM buffer, pH 7.2. (—) Ferric GHP before addition of riboflavin and EDTA and before irradiation; (- - -) after making the solution 22 μM in riboflavin and 1 mM in EDTA, but before irradiation; (· · · · ·) ferrous GHP and dihydroriboflavin generated by 5 min of photoreduction; (-·--·) 10 min after making the photoreduced solution 4.4 μM in H_2O_2. Arrow identifies the wavelength (450 nm) used to follow the reactions shown in (B). (B) Time courses of the peroxidation of dihydroriboflavin as followed by absorbance at 450 nm. a, 1.2 μM ferrous GHP-II, 22 μM dihydroriboflavin, and 2.8 μM H_2O_2; b, 1.2 μM ferrous GHP-II, 22 μM dihydroriboflavin, and 1.6 μM H_2O_2; c, 0.78 μM ferrous GHP-II, 15 μM dihydroriboflavin, and 1.9 μM H_2O_2.

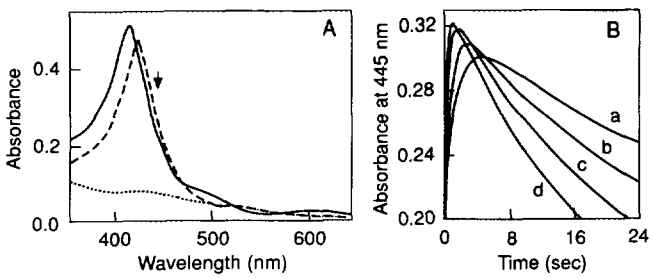

FIG. 4. Spectral detection of an intermediate in the H_2O_2-dependent bleaching of ferric GHP-I. (A) Spectra obtained with a 2.6 μM solution of ferric GHP-I in 50 mM buffer, pH 8.4, at 3°C. (—) Before the addition of H_2O_2; (- - -) 0.8 s after making the solution 16.2 mM in H_2O_2. (· · · · ·) 4 min after making the solution 16.2 mM in H_2O_2. Arrow identifies the wavelength (445 nm) used to follow the reactions shown in (B). (B) Time courses of the reaction as measured by absorbance at 445 nm. a, 2.0 mM H_2O_2; b, 4.1 mM H_2O_2; c, 8.1 mM H_2O_2; d, 16.2 mM H_2O_2.

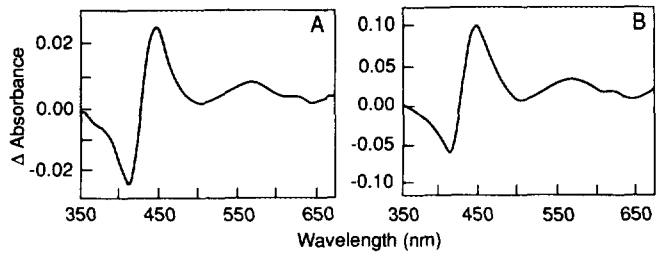

FIG. 5. Similarity of the spectral properties of Intermediate I formed from ferric GHP-I by addition of H_2O_2 and of ethyl hydroperoxide. Ferric GHP-I + peroxide minus ferric GHP-I difference spectra were recorded using 50 mM buffer, pH 8.4, at 3°C. (A) GHP-I (2.9 μM) 0.8 s after adding 8.1 mM H_2O_2. (B) GHP-I (1.7 μM) 4 s after adding 8.0 mM ethyl hydroperoxide.

concentration, that differs both from that of the starting ferric GHP-I (solid line) and from that of the final bleached products (dotted line). The difference spectrum resulting from intermediate formation is shown in Fig. 5A. When ethyl hydroperoxide replaces H_2O_2, an intermediate with similar spectral properties is formed (Fig. 5B). The reactions are perceived as proceeding according to the following scheme:

$$\text{GHP-Fe(III)} + \text{peroxide} \underset{k_{-1}}{\overset{k_1}{\rightleftharpoons}} \text{Intermediate I} \xrightarrow{k_2} \text{bleached products.} \quad [1]$$

Applying this scheme to the kinetic profiles (e.g., Fig. 4B), $k_1 = 170\ M^{-1}\ s^{-1}$, $k_{-1} = 1.3\ s^{-1}$, and $k_2 = 0.10\ s^{-1}$ were calculated for H_2O_2, and $k_1 = 23\ M^{-1}\ s^{-1}$, $k_1 = 2.6\ s^{-1}$, and k_2 of $0.68\ s^{-1}$ were calculated for ethyl hydrogen peroxide. Pseudo-Michaelis constants, $K'_m = (k_{-1} + k_2)/k_1$, were estimated to be 7.9 mM for H_2O_2 and 165 mM for ethyl hydroperoxide.

When ferrous GHP-I reacts with H_2O_2 at 17°C and pH 8.4, a triphasic reaction is observed (Fig. 6B). The first phase corresponds to the formation of "Intermediate II" (Fig. 6A), an intermediate which differs spectrally from Intermediate I (Fig. 4A). In the absence of suitable reductant, such as dihydroriboflavin, a fraction of Intermediate II rapidly undergoes bleaching, while the remainder is converted to a form that is spectrally indistinguishable from the ferric form, as reported previously (10); this form undergoes further bleaching in the presence of excess H_2O_2 as described above for ferric GHP-I. Figure 6A shows the spectra of the starting ferrous GHP-I (solid line), Intermediate II (dashed line, reconstructed from absorbance measurements taken at multiple wavelengths), and the product, with a spectrum like that of ferric GHP, generated from part of the intermediate (dotted line). We assume that the reaction of ferrous hemeprotein with H_2O_2 proceeds by the following scheme, where GHP-Fe(III) undergoes further bleaching:

$$\text{GHP-Fe(II)} + H_2O_2 \underset{k_{-1}}{\overset{k_1}{\rightleftharpoons}} \text{Intermediate II} \xrightarrow{k_2} \text{bleached products} + \text{ferric GHP-like product.} \quad [2]$$

Based on this assumption, kinetic parameters were calculated as $k_1 = 6.8 \times 10^4\ M^{-1}\ s^{-1}$, $k_{-1} = 6.8\ s^{-1}$, $k_2 = 1.4\ s^{-1}$, and $K'_m = 120\ \mu M$.

Spectrophotometric titration of GHP. The Soret bands of the ferric and ferrous forms of GHP-I and GHP-II were observed to shift toward longer wavelengths as the pH was increased during photometric titration from pH 3 to 11. For the ferric forms, two monoprotonic acid–base transitions occur at pH values of approximately 5 and 9; for the ferrous forms, a single monoprotonic acid–base transition occurs at approximately pH 5. These pK_a values derived from photometric titrations contrast (Table II) with the pK_a values of approximately 7 derived from mea-

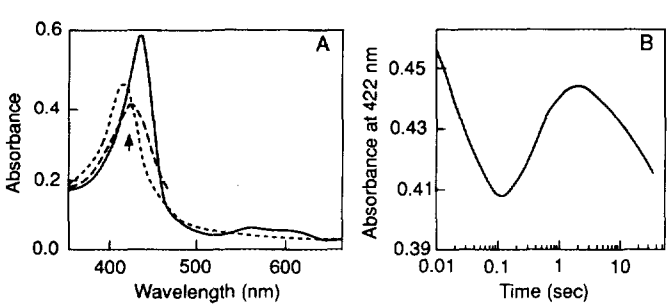

FIG. 6. Spectral detection of an intermediate in the H_2O_2-dependent bleaching of ferrous GHP-I. (A) Spectra obtained with a 3.1 μM solution of ferrous GHP-I in 10 mM buffer, pH 7.0, at 17°C under anaerobic conditions. (—) Ferrous GHP-I prepared from ferric form with a twofold molar excess of sodium dithionite; (- -) 0.125 s after making the solution 60 μM in H_2O_2; (- - -) 5 s after the solution was made 60 μM in H_2O_2. Arrow identifies the wavelength (422 nm) used to follow the reaction shown in (B). (B) Time course of the above reaction as measured by absorbance at 422 nm. The change of absorbance during the first 0.1 s is attributed to the formation of intermediate, the change between 0.1 and 2 s to the partial conversion of intermediate to the species with the ferric-like spectrum, and the change between 2 and 32 s to the further bleaching of this species by H_2O_2.

surements of the effect of pH on the secondary rate constants of ABTS peroxidative activity and of bleaching (Figs. 2B, 2C). Thus, the important acid–base transitions involved in the peroxidative activity are not demonstrated in the photometric titration of the unreacted GHP.

DISCUSSION

The reactions of peroxidases and myoglobin with H_2O_2 involve higher oxidation state intermediates (21–24). In the case of GHP, such intermediates are extremely unstable, making it difficult to measure kinetic parameters (10). The ability to couple the peroxidations of GHP to the oxidation of reductants provides the means for studying more readily the kinetics and mechanism of these peroxidative reactions. ABTS and dihydroriboflavin rapidly reduce the highly reactive and unstable intermediates that result when GHP and H_2O_2 react, thereby protecting GHP from destruction via the higher oxidation state intermediates. Moreover, the coupling reactions involving ABTS and dihydroriboflavin permit the measurement of the rate of intermediate formation. The rate constants obtained in this study for the formation of reactive oxygen species from HRP, metmyoglobin, and ferricytochrome c by the coupling methods are apparently valid since they agree with constants obtained previously by other methods (Table I).

Catalysis of ABTS peroxidation by ferric GHP is visualized as proceeding by reactions [3] + [4].

$$\text{GHP-Fe(III)} + \text{Peroxide} \rightarrow \text{Intermediate I} \quad [3]$$

$$\text{Intermediate I} + 2\ \text{ABTS} \rightarrow \text{GHP-Fe(III)} + 2\ \text{ABTS}^{+\cdot} \quad [4]$$

$$\text{Intermediate I} \rightarrow \text{Bleached Products} \quad [5]$$

In reaction [3] the hydroperoxide (H_2O_2 or ethyl hydroperoxide) generates a higher oxidation state of GHP, perhaps a perferryl intermediate, such as that seen with HRP and cytochrome c peroxidase (21–24, 26). In the absence of ABTS, the unstable Intermediate I leads to the generation of a bleached product via reaction [5]. Thus the H_2O_2-dependent bleaching of ferric GHP is visualized as proceeding by reactions [3] + [5]. In reactions [4], we perceive that two single-electron transfers from individual ABTS molecules to Intermediate I proceed in a consecutive way. Under the conditions of these experiments, we propose that Intermediate I formation (reaction [3]) is the rate-limiting step of both the catalysis of ABTS peroxidation (reaction [4]) and the hydroperoxide-dependent GHP bleaching reactions (reaction [5]). Moreover, we propose that ABTS prevents bleaching by reducing Intermediate I faster than the intermediate can undergo bleaching (that is, reaction [4] is faster than reaction [5]).

The kinetic findings support the above proposal. The coupled reaction is zero-order with respect to ABTS suggesting that under these conditions ABTS is saturating and intermediate formation, not ABTS oxidation, is rate limiting. The involvement of an intermediate in GHP bleaching is consistent with the double reciprocal kinetic plots previously reported (10). The rate constants determined for the coupled oxidation, the direct intermediate formation, and the bleaching reaction are quite similar if corrections are made for the differences in temperature (Table I). Moreover, the pH profiles of the ABTS peroxidation and H_2O_2-bleaching reactions are similar (Figs. 2B and 2C, Table II), suggesting that a common intermediate serves in these two reactions. The finding that H_2O_2 and ethyl hydroperoxide generate intermediates with indistinguishable spectra is also consistent with the formation of a common intermediate (Fig. 5).

Ferric GHP, like HRP, reacts with hydroperoxide to generate an intermediate that is reactive toward ABTS. The ABTS peroxidation reactions catalyzed by ferric GHP and HRP show stoichiometry of 2 ABTS oxidized/H_2O_2 consumed. Thus, the intermediates formed by reaction of ferric GHP with peroxide must be two oxidations states higher than the ferric state, as is the case with HRP. Intermediate I of GHP differs markedly from Compound I of HRP in terms of its spectral properties, stability, and rate of formation. Intermediate I of GHP shows an absorbance maximum at 426 nm (with an extinction comparable to that of ferric GHP) (Fig. 4A), in contrast to the 400-nm absorbance maximum of Compound I of HRP (21–24). The intermediate of GHP undergoes rapid bleaching, whereas HRP Compound I does not bleach. The rate constant for intermediate formation from H_2O_2 at neutral pH was approximately 10^4-fold greater with HRP than with GHP (Table I). The two proteins also differ with respect to the pH profiles of their ABTS peroxidation activities (Fig. 2, Table II). In contrast, the GHP intermediate does show spectral similarity to Compound ES of cytochrome c peroxidase (26).

In parallel to the ferric GHP-catalyzed peroxidation of ABTS, the ferrous GHP-catalyzed peroxidation of dihydroriboflavin is visualized as proceeding through Intermediate II by reactions [6] + [7]. H_2O_2-dependent bleaching of ferrous GHP is visualized as proceeding by reactions [6] + [8].

$$\text{GHP-Fe(II)} + H_2O_2 \rightarrow \text{Intermediate II} \quad [6]$$

$$\text{Intermediate II} + \text{Reduced Flavin} \rightarrow \text{GHP-Fe(II)} + \text{Oxidized Flavin} \quad [7]$$

$$\text{Intermediate II} \rightarrow \text{Bleached Products} + \text{GHP-Fe(III)} \quad [8]$$

We have no information as to whether reaction [7] proceeds as a single transfer of two reducing equivalents or by one-electron transfers. The product of the reaction is written as GHP-Fe(II) since GHP-Fe(III) is rapidly reduced by reduced flavin (10, 20). The formation of Intermediate II is apparently the rate-limiting step both in the

catalysis of dihydroflavin peroxidation and in the bleaching process. The rate constant of 2×10^4 M^{-1} s^{-1} determined by the coupled oxidation method for ferrous GHP-I agrees with the value obtained in the direct formation of Intermediate II (Table I). The observed rapid reaction of dihydroriboflavin with GHP Intermediate II is compatible with the hypothesis that intracellular dihydroflavin may react with higher oxidation states of hemeproteins, thereby diminishing the damage by these strong oxidants to cellular components (20, 31).

Whereas ferric GHP reacts with H_2O_2 at a rate much slower than does HRP, the reactions of ferrous GHP-I and GHP-II with H_2O_2 exhibit rate constants which are similar to the value of 10^5 M^{-1} s^{-1} for the reaction of ferrous HRP with H_2O_2 (27). The latter reaction generates Compound II that has been described as a ferryl-oxo derivative (21–23). The spectrum of Intermediate II observed upon mixing ferrous GHP-I and H_2O_2 (Fig. 6A) has an absorbance maximum at nearly the same wavelength as that of Compound II of HRP, suggesting a similarity between the two chromophores. However, Intermediate II of GHP differs from the ferryl derivative of HRP in that it is much less stable, undergoing a very rapid bleaching reaction.

The pK_a values derived from the kinetic pH profiles of the bleaching and coupling reactions of GHP differ from those derived from photometric titration (Table II), indicating that the protonations that change the spectra are not those that affect catalysis or bleaching reactions. The photometric titrations of many hemeproteins do not correspond to the pH profiles of their catalytic activities. An interesting possible explanation for the observed increase of rate constant in basic solution (Fig. 2B) would be general base catalysis of O–O cleavage of the heme-bound peroxide. Based on analogy with other hemeproteins, the pK_a values around 9 and 5 found in the photometric titrations of GHP might be attributable to a H_2O coordinated to the heme iron and to a nearby ionizable group of the protein, respectively (28–30).

Our studies demonstrate the peroxidative nature of the bleaching reaction of GHP and the efficiency of ABTS and dihydroflavin in reducing higher oxidation states of GHP. The reactions observed with the naturally occurring compound, dihydroflavin, as reductant may be important in protecting cells from oxidative damage. The peroxidative reactions contrast sharply with the reductase activity of the heme-free form of the protein (6) and illustrate the versatility of the protein.

ACKNOWLEDGMENTS

We thank Dr. Alfin Vaz for his ideas and critical reading of the manuscript.

REFERENCES

1. Morrison, M. (1961) *Nature* **189,** 765–766.
2. Hultquist, D. E., Dean, R. T., and Reed, D. W. (1976) *J. Biol. Chem.* **251,** 3927–3932.
3. DeFilippi, L. J., and Hultquist, D. E. (1978) *J. Biol. Chem.* **253,** 2946–2953.
4. DeFilippi, L. J., and Hultquist, D. E. (1978) *J. Biol. Chem.* **253,** 2954–2962.
5. DeFilippi, L. J., Toler, L. S., and Hultquist, D. E. (1979) *Biochem. J.* **179,** 151–160.
6. Xu, F., Quandt, K. S., and Hultquist, D. E. (1992) *Proc. Natl. Acad. Sci. USA* **89,** 2130–2134.
7. Yubisui, T., Matsuki, T., Takeshita, M., and Yoneyama, Y. (1979) *J. Biochem. (Tokyo)* **85,** 719–728.
8. Abe, Y., Ito, T., and Okazaki, T. (1990) *J. Biochem. (Tokyo)* **108,** 255–260.
9. Quandt, K. S., Xu, F., Chen, P., and Hultquist, D. E. (1991) *Biochem. Biophys. Res. Commun.* **178,** 315–321.
10. DeFilippi, L. J., Ballou, D. P., and Hultquist, D. E. (1979) *J. Biol. Chem.* **254,** 6917–6923.
11. Ko, K. M., and Godin, D. V. (1991) *Mol. Cell. Biochem.* **101,** 23–29.
12. Kanner, J., and Harel, S. (1985) *Arch. Biochem. Biophys.* **237,** 314–321.
13. Kaschnitz, R. M., and Hatefi, Y. (1975) *Arch. Biochem. Biophys.* **171,** 292–304.
14. O'Brien, P. J. (1969) *Can. J. Biochem.* **47,** 485–492.
15. Tappel, A. L., (1955) *J. Biol. Chem.* **217,** 721–733.
16. Galaris, D., Eddy, L., Arduini, A., Cadenas, E., and Hochstein, P. (1989) *Biochem. Biophys. Res. Commun.* **160,** 1162–1168.
17. Beaty, N. B., and Ballou, D. P. (1981) *J. Biol. Chem.* **256,** 4611–4618.
18. Massey, V., Stankovich, M., and Hemmerich, P. (1978) *Biochemistry* **17,** 1–8.
19. Childs, R. E., and Bardsley, W. G. (1975) *Biochem. J.* **145,** 93–103.
20. Xu, F., and Hultquist, D. E. (1991) *Biochem. Biophys. Res. Commun.* **181,** 197–203.
21. Dunford, H. B. (1982) *in* Advances in Inorganic Biochemistry (Eichhorn, G. L., and Marzilli, L. G., Eds) Vol. 4, pp. 41–68, Elsevier Biomedical, New York.
22. Hewson, W. D., and Hager, L. P. (1979) *in* The Porphyrins (Dolphin, D., Ed.), Vol. 7, pp. 295–332, Academic Press, New York.
23. Yamazaki, I., and Yokota, K. (1973) *Mol. Cell. Biochem.* **2,** 39–52.
24. Yonetani, T., and Schleyer, H. (1967) *J. Biol. Chem.* **242,** 1974–1979.
25. Radi, R., Thomson, L., Rubbo, H., and Prodanov, E. (1991) *Arch. Biochem. Biophys.* **288,** 112–117.
26. Yonetani, T. (1976) *in* The Enzymes (Boyer, P., Ed.) Vol. 13, pp. 345–362, Academic Press, New York.
27. Noble, R. W., and Gibson, Q. H. (1970) *J. Biol. Chem.* **245,** 2409–2413.
28. Brunori, M., Amiconi, G., Antonini, E., Wyman, J., Zito, R., and Fanelli, A. R. (1968) *Biochim. Biophys. Acta.* **154,** 315–322.
29. Theorell, H., and Akesson, A. (1941) *J. Am. Chem. Soc.* **63,** 1818–1820.
30. George, P., and Hanania, G. (1952) *Biochem. J.* **52,** 517–523.
31. Xu, F., and Hultquist, D. E. (1992) *Biochemistry* **31,** 2207. [Abstract]